APL Materials

Giant elastocaloric effect covering wide temperature range in columnar-grained $Cu_{71.5}Al_{17.5}Mn_{11}$ shape memory alloy

Cite as: APL Mater. 4, 106106 (2016); https://doi.org/10.1063/1.4964621
Submitted: 20 August 2016 • Accepted: 27 September 2016 • Published Online: 07 October 2016

Sheng Xu, Hai-You Huang, Jianxin Xie, et al.

Giant elastocaloric effect covering wide temperature range in columnar-grained $Cu_{71.5}Al_{17.5}Mn_{11}$ shape memory alloy

Sheng Xu,[1] Hai-You Huang,[1] Jianxin Xie,[1,a] Shouhei Takekawa,[2] Xiao Xu,[2] Toshihiro Omori,[2] and Ryosuke Kainuma[2,b]
[1]*Key Laboratory for Advanced Materials Processing of the Ministry of Education, University of Science and Technology Beijing, Beijing 100083, China*
[2]*Department of Materials Science, Graduate School of Engineering, Tohoku University, 6-6-02 Aoba-yama, Sendai 980-8579, Japan*

(Received 20 August 2016; accepted 27 September 2016; published online 7 October 2016)

The elastocaloric effect in a columnar-grained $Cu_{71.5}Al_{17.5}Mn_{11}$ shape memory alloy fabricated by directional solidification was investigated. A large entropy change of 25.0 J/kg K generated by the reversible martensitic transformation was demonstrated. The adiabatic temperature change of 12-13 K was directly measured, covering a wide temperature range of more than 100 K. The low applied stress with a specific elastocaloric ability of 100.8 K/GPa was identified and the potentially attainable operational temperature window as wide as more than 215 K was also discussed. The outstanding elastocaloric refrigeration capability, together with the low applying stress and uniform phase transformation, makes the columnar-grained Cu–Al–Mn shape memory alloy a promising material for solid-state refrigeration. [http://dx.doi.org/10.1063/1.4964621]

Solid-state refrigeration based on caloric effects (magnetocaloric, electrocaloric, barocaloric, and elastocaloric) has drawn significant attention in recent years due to its eco-friendliness as a promising alternative to conventional vapor compression, as well as its downscaling ability for microcooling.[1–5] Among all alternative non-vapor-compression technologies for refrigeration, elastocaloric refrigeration has been evaluated to be one of the most potential ways owing to its higher coefficient of performance and lower device cost.[6] Here, elastocaloric effect refers to the temperature change under adiabatic conditions of a given material during uniaxial loading or unloading, which is directly related to the isothermal entropy change of the reversible solid-to-solid phase transformation. Shape memory alloys (SMAs) undergo a reversible first-order diffusionless structure transition, making it capable of recovering inelastic deformation upon unloading. This property called pseudoelasticity is of particular interest for elastocaloric refrigeration as repeated loading-unloading cycles can be conducted for transporting heat. Compared with the magnetocaloric materials, SMAs for elastocaloric refrigeration show a larger reversible entropy change and an adiabatic temperature change, e.g., a temperature decrease of 17 K was observed for Ni–Ti wire during fast unloading,[7] as well as 6-7 K for Cu–Zn–Al polycrystalline sample.[8] Besides, the reversible martensitic transformation in SMAs is induced by uniaxial stress, which is easily controllable and relatively low in some alloys, for example, an applying stress of less than 100 MPa is simply required in Fe–Pd[9] and Ni–Mn–In–Co.[10] Moreover, high cyclic stability can be realized by tuning chemical composition and tailoring microstructure in SMAs; a Ni–Ti–Cu film was found to be capable of undergoing up to 10^6 cycles of stable elastocaloric refrigeration without functional fatigue.[11]

[a]E-mail address: jxxie@mater.ustb.edu.cn
[b]E-mail address: kainuma@material.tohoku.ac.jp

The refrigeration capability (RC) of a given elastocaloric material, which is frequently used as a key value for the evaluation of a refrigeration system, is defined as[2]

$$\mathrm{RC} = \int_{\omega_\mathrm{T}} \Delta S_\sigma (T)\, \mathrm{d}T, \tag{1}$$

where ΔS_σ is the entropy change governed by uniaxial stress and ω_T is the useful operational temperature window. Evidently, to achieve a strong refrigeration capability, ΔS_σ is expected to be large over a wide temperature range. Moreover, the adiabatic temperature change ΔT_{exp} via direct measurement is of importance for a more reliable and straightforward assessment of the field-induced thermal phenomena.[2]

A large stress-induced entropy change can be realized by a high level of applied strain before irreversible plastic deformation occurs.[5] Huge reversible strain can be achieved in single-crystalline SMAs, while it is difficult to be obtained in an ordinary polycrystalline one due to deformation incompatibility among separated grains.[12] The small reversible strain in polycrystalline SMAs strongly confines their applications in elastocaloric refrigeration. Fortunately, the reversible transformation strain can be significantly improved by microstructure tailoring in Cu–Al–Mn SMA with high cold-workability and machinability. Cu–Al–Mn-based SMAs with bamboo-like grains[13–15] or columnar grains[16,17] have shown enhanced pseudoelasticity and fatigue resistance. For a columnar-grained Cu–Al–Mn alloy, it shows a pseudoelasticity of more than 10%, which is comparable with that of single-crystalline one.[16] Therefore, it is expected that Cu–Al–Mn alloy exhibits an excellent elastocaloric effect. A single-crystalline $Cu_{72}Al_{17}Mn_{11}$ alloy was recently found to have a directly measured adiabatic temperature change of 3.9 K under compression, which is, however, not considerably large and is far away from the predicted value of 11.6 K due to the small achieved pseudoelasticity of less than 4%.[18] In this paper, we report on the elastocaloric effect in a columnar-grained $Cu_{71.5}Al_{17.5}Mn_{11}$ alloy under tension.

A $Cu_{71.5}Al_{17.5}Mn_{11}$ ingot with columnar-grained microstructure was prepared by directional solidification, and details can be found elsewhere.[17] Dog-bone-shaped tensile samples with a gauge size of 20 mm × 4 mm × 1 mm were cut out from the ingot with their length direction along the solidification direction (SD). The samples were first annealed at 1073 K for 5 min followed by quenching into ice water to obtain a single β_1 phase. Some of them were aged at 473 K for 15 min to stabilize the martensitic transformation temperatures. The grain orientation and morphology were investigated by the electron backscatter diffraction (EBSD) using a field emission scanning electron microscope (FE-SEM). The martensitic transformation temperatures and latent heat were determined by the differential scanning calorimeter (DSC) with a heating/cooling rate of 10 K/min, and the heat capacity was calibrated with a standard sapphire sample.

Tensile tests were conducted on a Shimadzu Autograph AG-X testing machine equipped with a thermostatic chamber. A cyclic tensile test at a strain level of 10% was carried out for the as-quenched sample at room temperature with a strain rate of 4.2×10^{-4} s^{-1}. For elastocaloric measurement, the temperature change of the sample was online monitored with a T-type thermocouple welded on the sample surface at a sampling frequency of 40 Hz, and the specific process is described as below. First, the applied strain was increased at a strain rate of 5.0×10^{-2} s^{-1} until reaching to exactly the set strain of 10% and held for 80 s to ensure that the sample temperature returned back to its origin value and then unloading at a strain rate of 1.3×10^{-1} s^{-1} to achieve a near-adiabatic condition.[19] Finally, the zero-stress status was kept for 120 s for the next loading-unloading cycle. Such a cycle was repeated for several times.

Fig. 1 shows the tensile stress-strain curve upon one loading-unloading cycle of the as-quenched sample tested at room temperature (~293 K). A fully reversible strain of 10% was observed. The stress-induced martensitic transformation occurred at 137 MPa, then the strain increased gradually by passing through a near-flat phase transformation plateau with a low gradient of appropriate 4.3 MPa/%, and reached 10% at a stress level of 183 MPa. The inset of Fig. 1 shows the quasi-colored orientation mapping microstructure of the as-quenched sample along SD and its corresponding color coding with a theoretical phase transformation strain contour line.[13] A strong ⟨100⟩ texture along SD was clearly identified as well as the straight grain boundary morphology, and the grain orientations along the transverse direction distributed randomly between ⟨100⟩ and

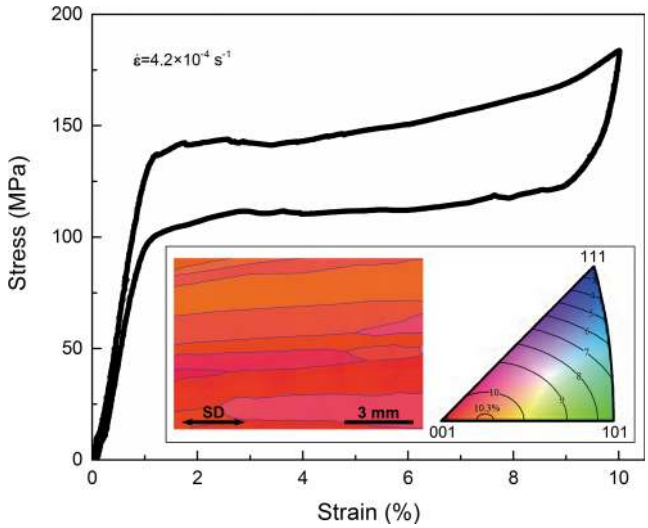

FIG. 1. Tensile stress-strain curve with a maximum applied strain of 10% at a room temperature for the as-quenched sample. The inset shows the quasi-colored orientation mapping microstructure of the as-quenched sample along SD and its corresponding color coding with a theoretical phase transformation strain contour line.

⟨110⟩.[16] The recovery strain due to pseudoelasticity is about 9% in Fig. 1, which is not far from the theoretical value.

The martensitic transformation starting temperature M_s, finishing temperature M_f, reverse transformation starting temperature A_s, and finishing temperature A_f of the as-quenched sample were measured to be 239 K, 228 K, 242 K, and 264 K, respectively. Fig. 2 shows the DSC curve upon heating of the as-quenched sample. The latent heat L released by the martensite-to-austenite transformation was determined to be 6400 J/kg, where the peak temperature T_{peak} was 256.2 K, and thus, the entropy change induced by the complete reversible phase transformation ΔS_{com} was calculated to be 25.0 J/kg K by

$$\Delta S_{com} = L/T_{peak}. \tag{2}$$

The ΔS_{com} has been demonstrated to show little dependence on temperature in a certain temperature range in Cu–Al–Mn alloy.[20] Then the ideal attainable adiabatic temperature change ΔT_{ideal} related to

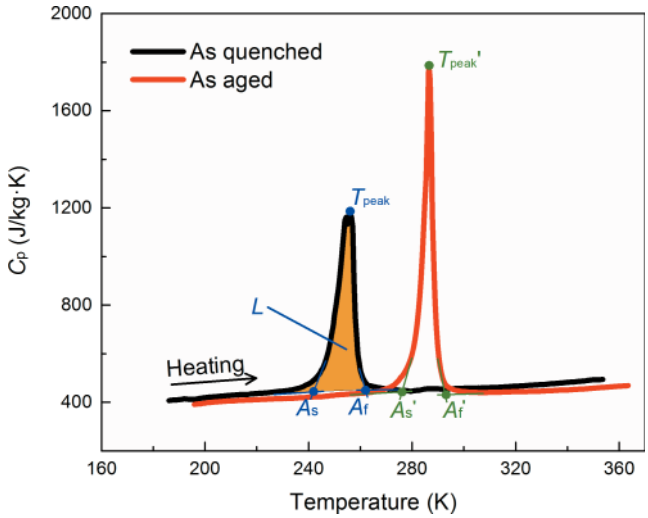

FIG. 2. DSC curve upon heating of the columnar-grained $Cu_{71.5}Al_{17.5}Mn_{11}$.

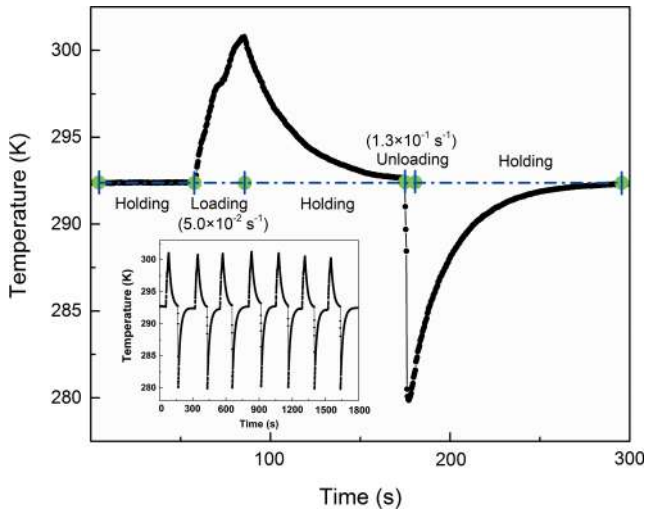

FIG. 3. Measured temperature of the as-quenched sample as a function of time during single loading-unloading cycle and the inset shows the temperature change vs time upon several loading-unloading cycles.

this entropy change could be calculated by[5]

$$\Delta T_{\text{ideal}} = \frac{T \cdot \Delta S_{\text{com}}}{C_{\text{p}}}, \tag{3}$$

where C_{p} is the heat capacity measured to be appropriate 455 J/kg K, and T is the testing temperature. Thus, the ΔT_{ideal} at a testing temperature of 293 K (around room temperature) was calculated to be 16.1 K. It is found that the large isothermal entropy change ΔS_{com} and its corresponding ideal adiabatic temperature change ΔT_{ideal} were comparable with or even higher than that of the reported Cu–Zn–Al,[5,8] indicating that a considerable potential of elastocaloric refrigeration is possessed in the present alloy.

A typical temperature change of the as-quenched sample during a single loading-unloading cycle is shown in Fig. 3. The testing temperature was room temperature and the maximum applied strain was set to be 10%. During loading at a strain rate of 5.0×10^{-2} s^{-1}, a temperature increase of ~8 K was observed, which was not the adiabatic temperature change because of the existence of temperature stabilization driven by the heat transfer between sample and environment. Then, the temperature went back to its origin value during holding at 10% strain for 80 s. Upon unloading, a near-adiabatic condition was achieved by the fast strain rate of 1.3×10^{-1} s^{-1}, and thus, a significant temperature decrease ΔT_{exp} of 12.8 K was measured, corresponding to the reverse transformation of the sample from the martensitic to the cubic phase when the stress was released. The inset of Fig. 3 shows the temperature change with several loading-unloading cycles, and a reproducible and stable adiabatic temperature change was demonstrated. It is surprisingly found that the ΔT_{exp} was relatively close to its ideal value at an approaching level of ~80% ($\Delta T_{\text{exp}}/\Delta T_{\text{ideal}}$ = 79.5%), which means that an almost complete isothermal entropy change was utilized in the elastocaloric process. We attribute this to the microstructure advantage of columnar-grained $Cu_{71.5}Al_{17.5}Mn_{11}$, the strong ⟨100⟩ texture as well as the straight grain boundary morphology contributed to an excellent deformation compatibility, and thus, a giant phase transformation strain of ~9% was successfully and reversibly achieved. This huge phase transformation strain reached ~90% of its maximum attainable value (~10%[13]) when stressed along ⟨100⟩ orientation, indicating that almost complete reversible martensitic transformation was actually processed. Also, it has been reported that it is beneficial to get a larger ΔT_{exp} when the stress was applied along the ⟨100⟩ orientation of certain elastocaloric alloys.[21] The slight difference between ΔT_{exp} and ΔT_{ideal} was caused by the imperfect adiabatic condition and a few residual untransformed austenite. The dissipated energy ΔW due to friction at the austenite/martensite interface should be also considered because it causes a negative impact on the measured adiabatic temperature change. The ΔW could be characterized by the area

of the hysteresis loop in the stress (σ)-strain (ε) curve,

$$\Delta W = \frac{\oint \sigma(\varepsilon)\mathrm{d}\varepsilon}{\rho}, \tag{4}$$

where ρ is the density. From the stress-strain curve in Fig. 1, the hysteresis loop area $\oint \sigma(\varepsilon)\mathrm{d}\varepsilon$ was calculated to be 3.48×10^6 J/m^3, and then the ΔW was determined to be 470 J/kg using $\rho = 7.40 \times 10^3$ kg/m^3.[22] Since the ΔW was involved in both loading and unloading processes, the dissipated energy-caused irreversible temperature change ΔT_{dis} during only unloading should be calculated using half of ΔW,

$$\Delta T_{\mathrm{dis}} = \frac{\Delta W}{2C_{\mathrm{p}}}, \tag{5}$$

where C_{p} is 455 J/kg K, and thereafter, ΔT_{dis} could be determined to be 0.52 K, and it can be said that the influence of dissipation energy by interfacial friction is very small because of the small hysteresis. This is one of the advantages of the Cu–Al–Mn SMA when compared to that of the Ni–Ti SMA with large hysteresis.

Since we have already identified a large ΔS_{com} and ΔT_{exp} in the columnar-grained $Cu_{71.5}Al_{17.5}Mn_{11}$, a wide operational temperature window is then highly required for a great refrigeration capability. We have thus checked the adiabatic temperature change of the columnar-grained $Cu_{71.5}Al_{17.5}Mn_{11}$ at different testing temperatures. Another as-quenched sample was first aged at 473 K for 15 min for stabilizing the martensitic transformation temperatures.[22] The isothermal entropy change $\Delta S'_{\mathrm{com}}$ of the as-aged sample was also determined by DSC to be 25.0 J/kg K, which was consistent with that of the as-quenched one, and the A'_{f} was about 295 K, as shown in Fig. 2. In order to not damage the sample, the start testing temperature was set to be 315 K, which was slightly higher than A'_{f}. The elastocaloric measurement was conducted at a step of 20 K, following the process described previously. It should be noticed that the same sample was used at each testing temperature; hence, the reversibility and reproducibility can be checked. The measured values of ΔT_{exp} were plotted in Fig. 4(a) as a function of testing temperature. It is found that a large and stable ΔT_{exp} of 12-13 K was obtained from 315 K to 418 K and that there was almost no reversible strain observed at 433 K resulting from the plastic deformation at a high temperature. Thus, within the range of measured testing temperatures, an operational temperature window ω_{T} from 315 K to 418 K covering a width of 103 K was successfully obtained. The inset of Fig. 4(a) shows the stress-strain curves upon loading at different testing temperatures of the as-aged sample and it is important to note that the large ΔT_{exp} was achieved at considerably low applying stresses. For example, the critical stress for inducing martensitic transformation was 83 MPa at 315 K in the as-aged sample, the maximum stress σ_{max} was 127 MPa, and the corresponding specific elastocaloric ability $\Delta T_{\mathrm{exp}}/\sigma_{\mathrm{max}}$ was then calculated to be 100.8 K/GPa, which is much higher than that of 22.7 K/GPa in Ni–Ti[7] and other elastocaloric alloys,[8,10,11,18,21,23–27] as shown in Fig. 4(b). The higher specific elastocaloric ability is beneficial for a higher coefficient of performance and more achievable device design for an elastocaloric refrigeration system;[28] this feature especially stands out when the testing temperature is close to the A_{f}. It also can be seen from Fig. 4(b) that the columnar-grained $Cu_{71.5}Al_{17.5}Mn_{11}$ displays a pretty higher ΔT_{exp} over most other elastocaloric alloys except Ni–Ti system.

We also compared the caloric performance of the as-aged columnar-grained $Cu_{71.5}Al_{17.5}Mn_{11}$ with other elastocaloric alloys,[8,10,21,23,26] as shown in Fig. 4(c). It is apparent that the present alloy has a high ΔT_{exp} over a considerably wide temperature range. Even though a wider temperature window was found for Fe–Pd[23] and Cu–Zn–Al,[8] the ΔT_{exp} (and ΔS_{com}) values for those two alloys are much lower than those of the present alloy. Using the obtained data, the corresponding RC was conservatively calculated by $\Delta S_{\mathrm{com}} \cdot \omega_{\mathrm{T}}$ to be ~2550 J/kg, which is higher than that of the reported Cu–Zn–Al,[8] suggesting a very strong refrigeration capability in the present alloy.

In addition, it should be mentioned that the martensitic transformation temperatures in the Cu–Al–Mn system are controllable by the adjustment of the chemical composition,[29] making it applicable to shift the operational temperature window towards practical application requirements. For example, $Cu_{68}Al_{17}Mn_{15}$ shows reversible stress-induced martensitic transformation even at a

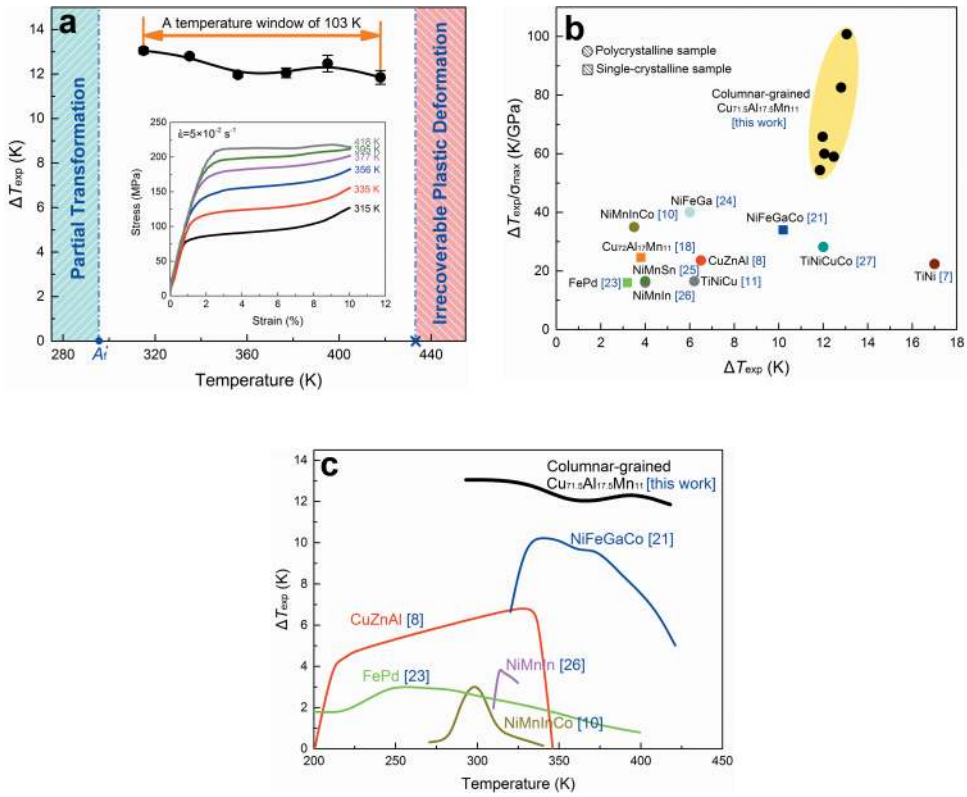

FIG. 4. (a) Measured adiabatic temperature change as a function of testing temperature for the elastocaloric effect in the as-aged columnar-grained $Cu_{71.5}Al_{17.5}Mn_{11}$. The inset shows the stress-strain curves upon loading at different testing temperatures. (b) A comparison of ΔT_{exp} and $\Delta T_{exp}/\sigma_{max}$ among the as-aged columnar-grained $Cu_{71.5}Al_{17.5}Mn_{11}$ at different testing temperatures and other elastocaloric alloys. (c) A comparison of caloric performance among the as-aged columnar-grained $Cu_{71.5}Al_{17.5}Mn_{11}$ and other elastocaloric alloys.

cryogenic temperature of 77 K.[21] More interestingly, for a columnar-grained Cu–Al–Mn alloy, the operational temperature window is feasible to be greatly enlarged based on the Clausius-Clapeyron relation,[30]

$$\frac{d\sigma_c}{dT} = -\frac{\Delta S_{com}}{V_m \cdot \varepsilon}, \tag{6}$$

where σ_c is the critical stress for inducing martensitic transformation, V_m is the molar volume, and ε is the strain caused by phase transformation. When a whole martensitic transformation is involved, the Cu–Al–Mn alloy displays the largest phase transformation strain when stressed along ⟨100⟩ orientation ($\varepsilon_{\langle 100\rangle} = \sim 10\% > \varepsilon_{\langle 110\rangle} = \sim 7.5\% > \varepsilon_{\langle 111\rangle} = \sim 2.0\%$[13]). Therefore, one can know that the columnar-grained Cu–Al–Mn alloy with a strong ⟨100⟩ texture shows a small $\frac{d\sigma_c}{dT}$. Using $\Delta S_{com} = 25.0$ J/kg K, $V_m = 7.6 \times 10^{-6}$ m^3/mol,[22] and $\varepsilon_{\langle 100\rangle} = \sim 10\%$, the $\frac{d\sigma_c}{dT}$ for the columnar-grained $Cu_{71.5}Al_{17.5}Mn_{11}$ was determined to be 1.85 MPa/K, which is smaller than that of 2.36 MPa/K in a bamboo-grained Cu–Al–Mn alloy with random textures,[22] as well as that of 5.56 MPa/K in polycrystalline Ni–Ti.[31] Assuming that the maximum attainable critical stress $\sigma_{c.max}$ is 450 MPa for a columnar-grained Cu–Al–Mn alloy[17] and using $\frac{d\sigma_c}{dT} = 1.85$ MPa/K, a very wide temperature window of ~243 K was calculated out. Subsequently, considering the thermal hysteresis ($A_f - M_s$) of ~25 K and that the lowest testing temperature should be just above A_f, a potentially attainable operational temperature window $\omega_{T.max}$ of more than 215 K was estimated to be obtained. For comparison, we put attention on commercial polycrystalline Ni–Ti regarding its $\omega_{T.max}$, using the maximum attainable critical stress as 800 MPa,[32] the temperature dependence of critical stress as 5.56 MPa/K,[31] and taking a stress hysteresis of ~200 MPa[32] into consideration, a value of 108 K was estimated for polycrystalline Ni–Ti. Then, it is easy to know that the $\omega_{T.max}$ for

columnar-grained Cu–Al–Mn is much wider than that of polycrylline Ni–Ti, implicating that a very strong elastocaloric refrigeration potential is possible to be tapped for columnar-grained Cu–Al–Mn alloy in the future.

Despite the strong refrigeration capability, the columnar-grained Cu–Al–Mn also takes other advantages as an elastocaloric material. Thanks to the uniform microstructure, the whole sample would share a compatible deformation during loading; thus, a uniform phase transformation can be induced upon stress,[16] which is vital to the improvement of the coefficient of performance of the elastocaloric refrigeration system.[28] Besides, the columnar-grained Cu–Al–Mn alloy has been reported to show reversible martensitic transformation in loading-unloading tensions upon 1000 cycles, exhibiting a higher cyclic stability than the ordinary polycrystalline counterparts.[17] However, compared to the Ni–Ti–Cu film with high cyclic stability,[11] the functional fatigue of the columnar-grained Cu–Al–Mn alloy leaves much to be desired, motivating us to improve its fatigue property in the following research.

In conclusion, a strong refrigeration capability was found in a columnar-grained $Cu_{71.5}Al_{17.5}Mn_{11}$ shape memory alloy due to the large reversible phase transformation-induced entropy change (ΔS_{com} = 25.0 J/kg K), giant directly measured adiabatic temperature change (ΔT_{exp} = 12-13 K), and wide operational temperature window (ω_T > 100 K). The excellent elastocaloric performance, together with the low cost, low applied stress ($\Delta T_{exp}/\sigma_{max}$ = 100.8 K/GPa), large potential operational temperature window ($\omega_{T.max}$ > 215 K), and uniform phase transformation, makes the columnar-grained Cu–Al–Mn shape memory alloy a promising candidate as an elastocaloric material for solid-state refrigeration.

This work was supported by the National Natural Science Foundation of China (Grant No. 51574027) and the National Key Research and Development Program of China (Grant No. 2016YFB0700505). S.X. wishes to thank the Direct Enrollment Education Programs, Center for International Exchange, Tohoku University, Japan for providing a scholarship.

[1] X. Moya, S. Karnarayan, and N. D. Mathur, Nat. Mater. **13**, 439 (2014).
[2] K. A. Gschneidner, Jr., V. K. Pechasky, and A. O. Tsokol, Rep. Prog. Phys. **68**, 1479 (2005).
[3] A. S. Mishenko, Q. Zhang, J. F. Scott, R. W. Wathmore, and N. D. Mathur, Science **311**, 1270 (2006).
[4] L. Mañosa, D. González-Alonso, A. Planes, E. Bonnot, M. Barrio, J. L. Tamarit, S. Aksoy, and M. Acet, Nat. Mater. **9**, 478 (2010).
[5] E. Bonnot, R. Romero, L. Mañosa, E. Vives, and A. Planes, Phy. Rev. Lett. **100**, 125901 (2008).
[6] W. Goetzler, R. Zogg, J. Young, and C. Johnson, *Energy savings potential and RD&D opportunities for non-vapor-compression HVAC technologies* prepared for U.S. Department of Energy (Navigant Consulting, Inc., 2014).
[7] J. Cui, Y. Wu, J. Muehlbauer, Y. Hwang, R. Radermacher, S. Fackler, M. Wuttig, and I. Takeuchi, Appl. Phys. Lett. **101**, 073904 (2012).
[8] L. Mañosa, S. Jarque-Farnos, E. Vives, and A. Planes, Appl. Phys. Lett. **103**, 211904 (2013).
[9] F. Xiao, T. Fukuda, and T. Kakeshita, Appl. Phys. Lett. **102**, 161914 (2013).
[10] B. Lu, F. Xiao, A. Yan, and J. Liu, Appl. Phys. Lett. **105**, 161905 (2014).
[11] C. Bechtold, C. Chluba, R. Lima de Miranda, and E. Quandt, Appl. Phys. Lett. **101**, 091903 (2012).
[12] S. M. Ueland and C. A. Schuh, J. Appl. Phys. **114**, 053503 (2013).
[13] Y. Sutou, T. Omori, K. Yamauchi, N. Ono, R. Kainuma, and K. Ishida, Acta Mater. **53**, 4121 (2005).
[14] T. Omori, T. Kusama, S. Kawata, I. Ohnuma, Y. Sutou, Y. Araki, K. Ishida, and R. Kainuma, Science **341**, 1500 (2013).
[15] Y. Sutou, T. Omori, R. Kainuma, and K. Ishida, Acta Mater. **61**, 3842 (2013).
[16] J. Liu, H. Huang, and J. Xie, Mater. Des. **64**, 427 (2014).
[17] J. Liu, H. Huang, and J. Xie, Mater. Des. **85**, 211 (2015).
[18] S. Qian, Y. Geng, Y. Wang, T. E. Pillsbury, Y. Hada, Y. Yamaguchi, K. Fujimoto, Y. Hwang, R. Radermacher, J. Cui, Y. Yuki, K. Toyotake, and I. Takeuchi, Philos. Trans. R. Soc., A **374**, 20150309 (2016).
[19] H. Ossmer, F. Lambrecht, M. Gültig, C. Chluba, E. Quandt, and M. Kohl, Acta Mater. **81**, 9 (2014).
[20] K. Niitsu, T. Omori, and R. Kainuma, Mater. Trans. **52**, 1713 (2011).
[21] F. Xiao, M. Jin, J. Liu, and X. Jin, Acta Mater. **96**, 292 (2015).
[22] Y. Sutou, N. Koeda, T. Omori, R. Kainuma, and K. Ishida, Acta Mater. **57**, 5759 (2009).
[23] F. Xiao, T. Fukuda, T. Kakeshita, and X. Jin, Acta Mater. **87**, 8 (2014).
[24] Y. Xu, B. Lu, W. Sun, A. Yan, and J. Liu, Appl. Phys. Lett. **106**, 201903 (2015).
[25] W. Sun, J. Liu, B. Lu, Y. Li, and A. Yan, Scr. Mater. **114**, 1 (2016).
[26] Y. Huang, Q. Hu, N. M. Bruno, J. Chen, I. Karaman, J. H. Ross, Jr., and J. Li, Scr. Mater. **105**, 42 (2015).
[27] H. Ossmer, C. Chluba, M. Gueltig, E. Quandt, and M. Kohl, Shape Mem. Superelasticity **1**, 142 (2015).
[28] S. Qian, Y. Geng, Y. Wang, J. Ling, Y. Hwang, R. Radermacher, I. Takeuchi, and J. Cui, Int. J. Refrig. **64**, 1 (2016).
[29] R. Kainuma, S. Takahashi, and I. Ishida, Metall. Mater. Trans. A **27**, 2187 (1996).
[30] P. Wollants, M. De Bonte, and J. R. Roos, Z. Metallkd. **70**, 113 (1979).
[31] T. Omori, K. Ando, M. Okano, X. Xu, Y. Tanaka, I. Ohnuma, R. Kainuma, and K. Ishida, Science **333**, 68 (2011).
[32] K. Otsuka and X. Ren, Prog. Mater. Sci. **50**, 511 (2005).